A MIMO Robust Design of a PID for Refrigeration Systems based on Vapour Compression

M. Tari and P. Lanusse

Bordeaux INP, IMS CNRS UMR 5218, France
Université de Bordeaux, IMS CNRS UMR 5218, France
(e-mail: surname@ims-bordeaux.fr)

Abstract: In this paper, an original method for the design of PID Controller for MIMO application is presented. The proposed method is based on the CRONE MIMO approach which makes easier the design of MIMO robust controllers. The problem treated here is the control of a refrigeration system based on vapour compression in order to achieve high energy efficiency and to satisfy the cooling demand. Simulation results show the good control performance and robust stability for a wide set of operating points.

Keywords: Refrigeration systems, Robust control, MIMO system, CRONE control design, Fractional Order PID

1. INTRODUCTION

1.1 *Fractional PID controller*

The Proportional, Integral and Derivative (PID) controller is widely used in industrial application. It ensures speed, accuracy and stability degree performance. A parallel form of the PID controller is often proposed for an output feedback (Fig.1):

$$C(s) = C_P + \frac{C_I}{s} + C_D s\,, \tag{1}$$

A series form of the PID controller could be easier to design:

$$C(s) = C_0 \left(1+\frac{\omega_I}{s}\right) \frac{1+s/\omega_1}{1+s/\omega_2} \frac{1}{1+s/\omega_F}. \tag{2}$$

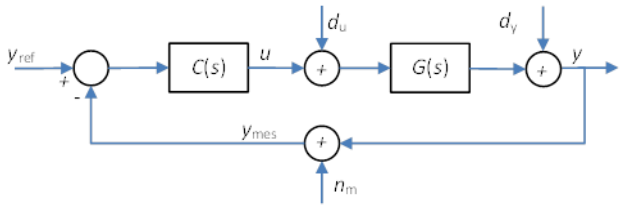

Fig. 1. Unity-feedback configuration

Each term is band-limited and ensures one of the controller behaviour: proportional, integral, derivative and filtering. The low-pass filter has been added to make the controller strictly proper and thus to ensure a decreasing gain of the control sensitivity function.

Replacing the Laplace variable s by fractional power of s, parallel PID (1) becomes a PI$^{\lambda}$D$^{\mu}$ that should be defined by:

$$C(s) = C_P + \frac{C_I}{s^{\lambda}} + \frac{C_D s^{\mu}}{1+\tau_F s^{\gamma}}, \tag{3}$$

Through the two more parameters λ and μ, this controller offers a better flexibility than the conventional PID and the constant τ_F avoids that the control sensitivity function tends towards infinity. Depending on the value of γ, $C(s)$ is biproper for $\gamma = \mu$ and strictly proper for $\gamma > \mu$.

In order to simplify its design and implementation, it is possible to choose a fractional order PID controller defined by:

$$C(s) = C_0 \left(1+\frac{\omega_I}{s}\right)^{n_I} \left(\frac{1+\frac{s}{\omega_1}}{1+\frac{s}{\omega_2}}\right)^{\mu} \frac{1}{\left(1+\frac{s}{\omega_F}\right)^{n_F}}, \tag{4}$$

with $\omega_I \le \omega_1 \le \omega_2 \le \omega_F$ and $n_I \in \mathbb{N}$, $\mu \in \mathbb{R}$, $n_F \in \mathbb{N}$. Fig. 2 presents a Bode plot of this PID$^{\mu}$(F) controller. For $\gamma = \mu$, $\lambda = n_I$, the corner frequencies of (3) can be approximated by:

$$\omega_I = \left(\frac{C_I}{C_P}\right)^{1/\lambda}, \ \omega_1 = \left(\frac{C_P}{C_D + C_P\tau_F}\right)^{1/\mu} \text{ and } \omega_2 = \left(\frac{1}{\tau_F}\right)^{1/\gamma} \tag{5}$$

Fractional order PID has been the subject of considerable interest among researchers who have developed a large number of tuning techniques (Podlubny 1999a-b, Chen 2004, Petras 1999, Nataraj 2007, Monje 2010, etc.). This interest is due mainly to the usual belief that "fractional" leads necessarily to an improved performance, mainly in terms of robustness. Nevertheless, the fractional order PID designs do not explicitly take into account a well-defined perturbation model of the plant. At the opposite, the fractional order CRONE design methodology is based on the perturbed model in order to ensure both performance and robustness.

1.2 *CRONE Control-System Design (CSD) methodology*

The CRONE (a french acronym which means fractional order robust control) CSD methodology is a frequency-domain approach developed since the eighties (Oustaloup 1983,

1991, 1995; Lanusse, 1994). It is based on the common unity-feedback configuration presented by Fig. 1. Three CRONE CSD methods have been developed. Each of them denotes a generation of CRONE design. The first two are based on a real fractional order and ensure a good robustness for plant gain variations.

The first generation CRONE controller is defined within a frequency range [ω_A, ω_B] around the desired open-loop gain crossover frequency ω_{cg} from the fractional transfer function of an order n integro-differentiator. To manage the control effort level and steady state errors, the CRONE controller includes a band-limited integrator and low-pass filter. It is defined by relation (4) with $\omega_{cg}=\sqrt{\omega_1\omega_2}$. Around ω_{cg} the constant controller phase $\mu\pi/2$ ensures the constancy of the phase margin when the plant phase is constant both versus frequency and plant parameters. The achievable rational version of this controller can be obtained using the Oustaloup's approximation (Oustaloup 1983, 1991).

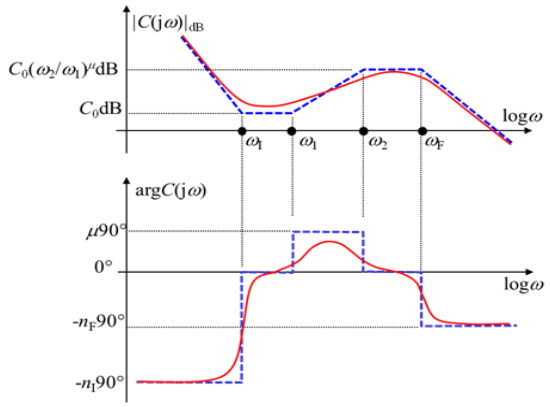

Fig. 2. Frequency response of a series fractional order PID$^{\mu}$(F) controller for: $n_l=2, n_F=1$ and $\mu=0.75$

The second CRONE CSD generation can be used even if the plant phase varies versus the frequency. It uses a nominal open-loop transfer function that includes a band-limited fractional order integrator.

The third generation extends the field of application of the second one and should be used for any kind of plant perturbation model. The nominal open-loop (for the nominal plant G_0) is defined by:

$$\beta_0(s)=\beta_l(s)\beta_m(s)\beta_h(s), \tag{6}$$

- where $\beta_m(s)$ is a set of band-limited complex fractional order integrators:

$$\beta_m(s)=\prod_{k=-N^-}^{N^+}\beta_{mk}(s), \tag{7}$$

with:

$$\beta_{mk}(s)=C_k^{\mathrm{sign}(b_k)}\left(\alpha_k\frac{1+s/\omega_{k+1}}{1+s/\omega_k}\right)^{a_k}\left(\Re e_{/i}\left\{\left(\alpha_k\frac{1+s/\omega_{k+1}}{1+s/\omega_k}\right)^{ib_k}\right\}\right)^{-q_k\mathrm{sign}(b_k)}$$

$$\alpha_k=(\omega_{k+1}/\omega_k)^{1/2}\ \text{ for } k\neq 0 \text{ and } \alpha_0=\left(1+\left(\frac{\omega_r}{\omega_0}\right)^2\Big/1+\left(\frac{\omega_r}{\omega_1}\right)^2\right)^{1/2} \tag{8}$$

- where $\beta_l(s)$ is an integer order n_l proportional integrator and where $\beta_h(s)$ is a low-pass filter of integer order n_h:

$$\beta_l(s)=C_l\left(\frac{\omega_{-N^-}}{s}+1\right)^{n_l},\ \beta_h(s)=C_h\left(\frac{s}{\omega_{N^+}}+1\right)^{-n_h}. \tag{9}$$

Gains C_x (C_k, C_l and C_h) are such that ω_r is the nominal closed-loop resonant frequency. Order n_l has to be set to manage the accuracy provided by the control-system. Order n_h has to be set to obtain a bi-proper or strictly-proper controller.

When $N^+ = N^- = 0$, only four open loop parameters are optimized in order to minimize a robustness cost function J:

$$J=\sup_G\left|M_T\right|-M_{T0}, \tag{10}$$

where M_{T0} is a required value of the nominal resonant peak of the complementary sensitivity function $T(s)$. To manage precisely performance related to tracking, regulation and control effort level, 5 inequality constraints are to be fulfilled for all plants (or parametric states of the plant):

$$\inf_G\left|T(j\omega)\right|\geq T_l(\omega),\ \sup_G\left|T(j\omega)\right|\leq T_u(\omega),\ \sup_G\left|S(j\omega)\right|\leq S_u(\omega)$$

$$\sup_G\left|CS(j\omega)\right|\leq CS_u(\omega)\ \text{and}\ \sup_G\left|SG(j\omega)\right|\leq SG_u(\omega), \tag{11}$$

$$\text{with}\quad \begin{cases} T(s)=\dfrac{G(s)C(s)}{1+G(s)C(s)} & S(s)=\dfrac{1}{1+G(s)C(s)} \\ CS(s)=\dfrac{C(s)}{1+G(s)C(s)} & SG(s)=\dfrac{G(s)}{1+G(s)C(s)} \end{cases}. \tag{12}$$

The optimal open-loop parameters position the open-loop frequency uncertainty domains –defined by possible values of $G(j\omega)/G_0(j\omega)$– in order to not overlap the low stability margin areas of the Nichols chart. The parameterization of the nominal open-loop transfer function by complex fractional orders simplifies the optimization considerably. During optimization a complex order has the same function as a whole set of parameters found in common rational controllers. When it is useful, N^- and N^+ are different from 0 to increase the number of tuning parameters.

Then, the fractional controller $C_F(s)$ is defined by its frequency response:

$$C_F(j\omega)=\frac{\beta_0(j\omega)}{G_0(j\omega)}. \tag{13}$$

Finally, this desired frequency response is fitted by a low order rational transfer function $C_R(s)$. When the objective is to design a PID, an order 3 rational transfer function is tuned. In other words, a robust PID controller can also be designed by using the third generation CRONE design methodology. A CRONE CSD toolbox is downloadable for free (Lanusse, 2010).

1.3 *Refrigeration system based on vapour-compression*

The non-linear MIMO system to be controlled is a refrigeration system based on vapour compression (Bejarano, 2017). This system (Fig 3) requires 4 components: a compressor, condenser, expansion valve, and evaporator. The compressor compresses the refrigerant to a high pressure and

high temperature and then flows to the condenser, which is a heat exchanger where heat is rejected to the environment. The refrigerant is condensed to a liquid. The hot liquid refrigerant then passes through an expansion valve, where the refrigerant expands to a low pressure and a low temperature. The cold refrigerant then flows through the evaporator, where it absorbs heat and boils back into a vapour on its way back to the compressor. Two variables: the outlet temperature of the evaporator secondary flux $T_{e,sec,out}$ (which represent the cooling demand) and the degree of superheating T_{SH} are to be controlled by manipulating two variables: the compressor speed N and the expansion valve Av and by considering also the disturbances. The coefficient of performance COP is used as quality steady-state performance variable, which defined as the ration between the cooling power generated at the evaporator and the mechanical power provided by the compressor. The model is controlled with a sampling period equals to 1 second.

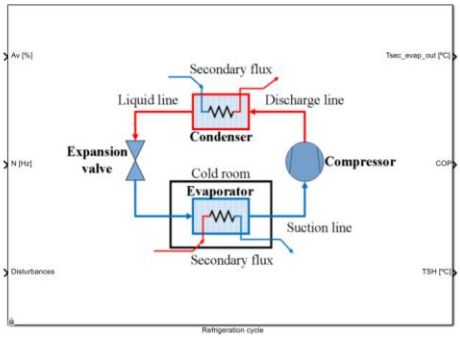

Fig. 3. Simulink block describing the refrigeration process

2. CRONE APPROACH FOR MIMO SYSTEMS

2.1 *CRONE Control-System Design (CSD) methodology*

The CRONE methodology has been extended to control a MIMO mxn system $\mathbf{G}$ (n inputs, m outputs) (Lanusse *et al.*, 1996, 2000, 2016; Sutter, 1997, Sabatier *et al.*, 2015). The main objective is to determine nxm controller $\mathbf{C}$ that ensures the perfect decoupling of the closed-loop complementary sensitivity function $\mathbf{T}_0$ for the nominal plant model $\mathbf{G}_0$. Thus the nominal open-loop transfer function is diagonal and is defined by:

$$\boldsymbol{\beta}_0(s) = \mathbf{G}_0(s)\mathbf{C}(s) = \begin{bmatrix} \beta_{0\,11}(s) & \cdots & 0 \\ \vdots & \ddots & \vdots \\ 0 & \cdots & \beta_{0\,mm}(s) \end{bmatrix} \quad (11)$$

Each element of $\boldsymbol{\beta}_0(s)$ is based on the third generation CRONE SISO methodology as described in section *1.2*. Parameters of all $\beta_{0ii}(s)$ are optimized together in order to stabilize the nominal closed-loop and to minimize the resonant peak variation of all $T_{ii}(s)$. Once $\boldsymbol{\beta}_0(s)$ has been optimized, the controller is obtained from

$$\mathbf{C}(s) = \mathbf{G}_0^{*}(s)\boldsymbol{\beta}_0(s) = \begin{bmatrix} C_{11}(s) & & C_{1m}(s) \\ & \ddots & \\ C_{n1}(s) & & C_{nm}(s) \end{bmatrix} = \left[C_{ij}(s)\right] \quad (12)$$

where $\mathbf{G_0}^{*}(s)$ is $\mathbf{G_0}^{-1}(s)$ the inverse matrix of $\mathbf{G_0}(s)$ when $m = n$, or $\mathbf{G_0}^{\dagger}(s)$ the Moore-Penrose pseudo-inverse matrix of $\mathbf{G_0}(s)$ in the case when $m \neq n$. To ensure the system stability, the nominal open-loop transfer function should include some time-delays and poles and zeros in the right half-plane and lightly damped modes which appear in $\mathbf{G_0}^{*}(s)$ and $\mathbf{G_0}(s)$ (Nelson-Gruel *et al.*, 2008, Sabatier *et al.*, 2015, Lanusse *et al.*, 2016). This methodology provides an efficient MIMO controller, but may be sometimes difficult to use: taking into account all the features of $\mathbf{G_0}^{*}(s)$ and $\mathbf{G_0}(s)$ could be cumbersome. Thus, when a RGA analysis proves it (Sabatier *et al.,* 2015), LTI square mxm MIMO uncertain plants can be controlled using decentralized (diagonal) MIMO controllers.

2.1.1 *MIMO design of a decentralized controller*

A decentralized controller can be obtained by choosing an arbitrary diagonal model for $\mathbf{G_0}(s)$. Nevertheless, the MIMO features of $\mathbf{G}$ are taken into account at the time of MIMO open-loop optimization as for instance they contribute to the resonant peak variation of all perturbed $T_{ii}(s)$ (Lamara 2012). Thus, the parameters of all $\beta_{0ii}(s)$ need to be optimized at the same time.

2.1.2 *Multi-SISO design of a decentralized controller*

When the plant is diagonal dominant, the multi-SISO CRONE approach can be used to design a decentralized controller (Sutter, 1997, Lanusse, 2010) This approach enables an independent tuning of each open-loop transfer function $\beta_{0ii}(s)$ (thus of each $C_i(s)$) by taking into account the diagonal nominal transfer function $G_{ii0}(s)$ and an uncertainty defined by the structured uncertainty coming from all possible values $G_{ii}(s)$ enlarged by an unstructured uncertainty computed from modulus of column off-diagonal terms $G_{ji}(s)$.

3. MIMO PLANT ANALYSIS

The MIMO refrigeration system needs to be analysed to know what kind of controller and control system design methodology can be used. For this purpose, several tools can be used: Relative Gain Array Analysis (RGA), Column Diagonal Dominance Degree (CD^3). But, first of all, in order to use these tools, the previous described system needs to be linearized.

3.1 *System linearization*

The refrigeration system is linearized around 9 operating points (blue points in fig. 4) chosen in the space of the controlled variables (Bejarano, 2017).

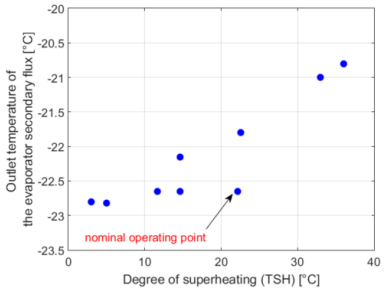

Fig. 4. Operating points used for system linearization

The obtained frequency responses are represented on Fig. 5. The nominal operating point is arbitrary defined by Plant #2 located on Fig. 4. Each input-output transfer function is described by: G_{11}: from Av (%) to $T_{e,sec,out}$ (°C); G_{12}: from N

(Hz) to $T_{e,sec,out}$ (°C); G_{21}: from Av (%) to T_{SH} (°C); G_{22}: from N (Hz) to T_{SH} (°C). From Fig.5, we can notice variations of frequency responses due to the nonlinearities of the system. Thus, these nonlinearities will be taken into account in the controller design.

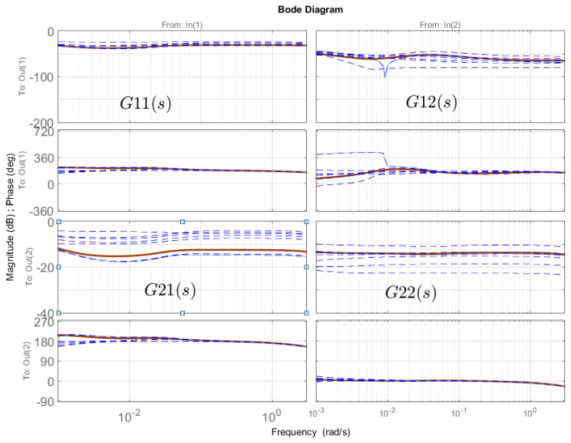

Fig. 5. Bode diagram of nominal plant frequency response (solid brown curves) and all operating point frequency responses (blue dashed curves)

3.2 *RGA and CD³ analysis*

The RGA tool quantifies the relationship between an input and an output and expresses how the output can be modified by the other inputs. It shows the coupling level of a system and if a decentralized control could be efficient. For a given mxm plant $\mathbf{G}$, the RGA matrix $\mathbf{\Lambda}$ is obtained from:

$$\mathbf{\Lambda}(\mathbf{G}(j\omega)) = \mathbf{G}(j\omega) \circ \left(\mathbf{G}^{-1}(j\omega)\right)^{T} = \left[\lambda_{ij}(j\omega)\right] \quad \text{with } i \text{ and } j \le m\,, \tag{13}$$

For the considering MIMO system, Fig. 6 shows that for the 9 operating points, $\lambda_{11}(j\omega)$ and $\lambda_{22}(j\omega)$ are close to 1 and greater than $\lambda_{12}(j\omega)$ and $\lambda_{21}(j\omega)$ along the studied frequency range. Thus a decentralized controller can be efficient to control the plant.

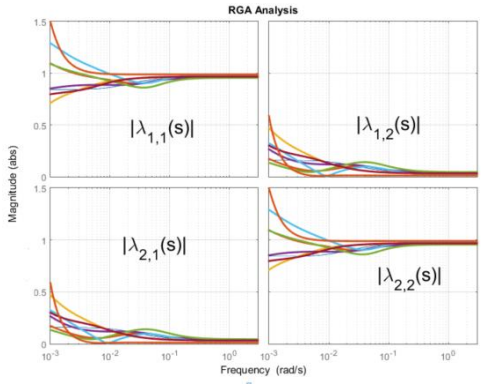

Fig. 6. Magnitude of diagonal and off-diagonal elements of the RGA matrices of $\mathbf{G}$

The CD³ tool compares, column by column, the magnitude of each diagonal element G_{ii} of $\mathbf{G}$ to the sum of the magnitude of the off-diagonal elements G_{ji} with $j \neq i$. Fig.5 shows that $|G_{22}|$ is greater than $|G_{21}|$ but $|G_{11}|$ is lower than $|G_{21}|$. Which means that, an efficient $C_2(s)$ can be designed by using the CRONE multi-SISO approach to control output y_2 of Fig.7.

At the opposite, designing $C_1(s)$ by using the multi-SISO approach would provide a conservative controller for output y_1. Nevertheless, $C_1(s)$ can be designed by using the SISO approach and by taking into account the equivalent plant $G_{11}^{*}(s)$ defined by $Y_1(s)/U_1(s)$ with $U_2(s) = -C_2(s)Y_2(s)$.

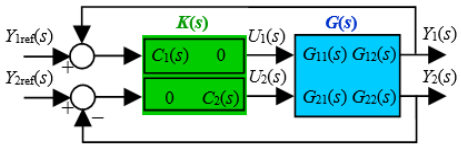

Fig. 7. Decentralized control of a 2x2 MIMO plant

4. DESIGN OF A DECENTRALIZED CRONE CONTROLLER

4.1 *Multi-SISO CRONE design of $C_2(s)$ controller*

Fig.8.a shows the Nichols plot of G_{22} whose uncertainty frequency domains have been enlarged by taking into account the off-diagonal elements G_{12} of $\mathbf{G}$.

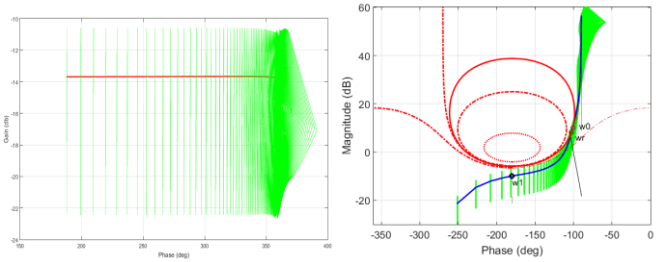

Fig. 8 (a) Nichols plot of G_{22} of $\mathbf{G}$: nominal frequency responses (—); enlarged uncertainty domains (—); (b) Nichols plot of β_{022} nominal frequency response (—); enlarged uncertainty domains (—); 0.1 dB M-contour related to M_{T0} (—)

By taking into account the enlarged uncertainty, $\beta_{022}(s) = C_2(s)G_{022}(s)$ is tuned. The desired closed-loop bandwidth is 0.5 rad/s. Fig. 10 shows the frequency domain constraints and the nominal and extreme values of the optimal sensitivity functions The required resonant peak M_{T0} is 0.1 dB, the resonant peak limitation (T) is 2dB. In order to ensure a fast convergence of the output towards the input, the sensitivity function T is chosen very close to 0dB at low frequency (-0.1dB <T <0.1 dB). The sensitivity function limitation (S) is 6dB and the plant input sensitivity function limitation (SG) is -5dB. The control effort sensitivity function limitation (CS) is 25dB. The low frequency order n_{l2} of the nominal fractional open loop needs to be 1. To limit the control effort sensitivity at high frequency and to obtain a strictly proper controller, the high frequency order n_{h2} needs to be 2. The 4 optimized parameter values for β_{022} are: $Y_{r2} = 9.95$ dB; $\omega_{r2} = 0.09$ rad/s; $\omega_{02} = 0.119$ rad/s; $\omega_{l2} = 2.16$ rad/s. Thus, $a_{02} = 1.08$, $b_{02} = 0.42$ and $K_2 = 2.72$. Fig. 8.b presents the Nichols plot of the optimized open loop frequency response $\beta_{022}(s)$. The final value of the cost function J is 0.12 dB and all sensitivity constraints are met (Fig. 9.a). Finally, by using relation (13) we obtain the fractional version of $C_2(s)$ whose frequency response is fitted by an order 3 PID-like rational transfer function:

$$C_2(s) = \frac{8.063s^2 + 8.361s + 1.616}{1.253s^3 + 5.025s^2 + s}\,. \tag{14}$$

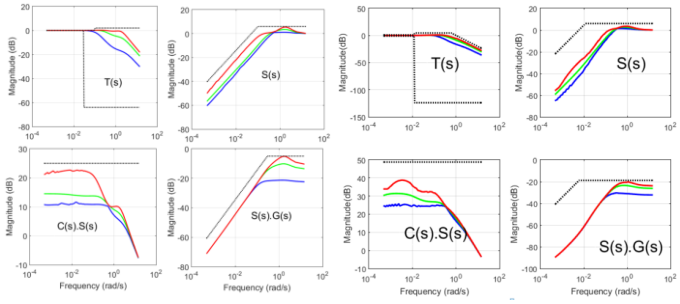

Fig. 9 Frequency-domain constraints (---) on perturbed values of $|T(j\omega)|$, $|S(j\omega)|$, $|CS(j\omega)|$ and $|SG(j\omega)|$: (left) for controller C_1; (right) for controller C_2;

4.2 *SISO CRONE design of $C_1(s)$ controller*

The nominal open-loop transfer function $\beta_{011}(s) = C_1(s)G_{011}^*(s)$ is designed by taking into account the equivalent plant $G_{11}^*(s)$ which includes the controller $C_2(s)$:

$$G_{11}^*(s) = G_{11}(s) - \frac{G_{21}(s)C_2(s)G_{12}(s)}{1+C_2(s)G_{22}(s)}. \qquad (15)$$

Fig.10.a shows the Nichols plot of $G_{11}^*(s)$.

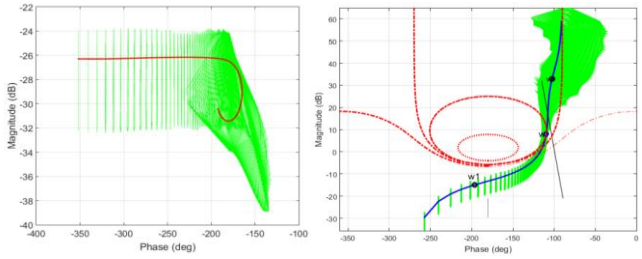

Fig. 10 (a) Nichols plot of G_{11}^*: nominal frequency response (—); uncertainty domains (—); (b) Nichols plot of β_{011} nominal frequency response (—); uncertainty domains (—); 0.5 dB M-contour related to M_{T0} (—)

For β_{011}, the required resonant peak M_{T0} is 0.5 dB, the resonant peak limitation (T) is 4.5dB, the sensitivity function limitation (S) is 6dB and the plant input sensitivity function limitation (SG) is -19dB. The optimized parameters values are: Y_{r1} = 9.95 dB; ω_{r1} = 0.1 rad/s; ω_{01} = 0.009 rad/s; ω_{11} =2 rad/s, n_{l1} = 1, n_{h1} = 2 and. Thus, a_{01} = 1.13, b_{01} = 0.24 and K_1 = 40.7. The final value of the cost function J is 0.37dB. Fig. 10.b and 9.b present the Nichols plot of the optimized open loop frequency response $\beta_{011}(s)$ and the sensitivity constraints. The PID-like rational form of $C_1(s)$ is:

$$C_1(s) = \frac{-428s^2 - 475.9s - 14.79}{42.26s^3 + 98.47s^2 + s} \qquad (16)$$

4.3 *Linear framework evaluation of the CRONE decentralized controller*

Fig.11 shows the step responses of the closed-loop linear system (9 operating points) for step variations of the reference signals. As we can observe, the plant outputs are both stable and damped: the percentage overshoots are always lower than 20%. As for the coupling effects, both disturbances are rejected.

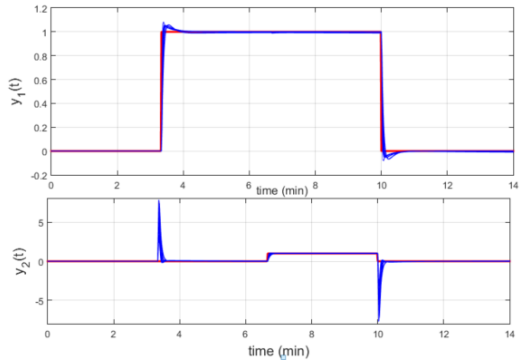

Fig. 11 Variations of y_1 and y_2 (—) for step variations of $y_{ref\,1}$ and $y_{ref\,2}$ (—)

5. SIMULATION RESULTS

5.1 *Evaluation results*

A standard simulation have been performed using the model defined in section 1. This simulation, includes step changes in the input signals references on $T_{e,sec,out}$ and T_{SH} and in the most important disturbances: the inlet temperature of the evaporator secondary flux $T_{e,sec,in}$ and the inlet temperature of the condenser secondary flux $T_{e,sec,in}$. A sampling time of 1 second is considered. Fig. 12 presents the results of the standard simulation using the decentralized CRONE controller described in section 4. It shows that the plant outputs are stable and well damped: the percentage overshoots are always less than 20%.with the respect to the input references and a settling time less than 30s. Moreover, it is important to observe that the plant outputs are decoupled and the disturbances are well rejected.

5.2 *Comparing multivariable controllers*

In this subsection, the CRONE decentralized controller is compared with the default PID decentralized controller described in (Bejarano, 2017). On Fig 12, we appreciate that the better response of $T_{e,sec,out}$ and T_{SH} are reached with the CRONE controller and this for a fairly close control effort level compared with the one of the default PID controller. Moreover, for a quantitative comparison eight individual performance indices and one combined index are evaluated (Bejarano, 2017). The numerical values of the evaluated indices are presented on Table 1. As we can see, all the indices quantifying the error signals for the CRONE controllers are better than those of the benchmark controller.

Table 1. Relative indices and the combined index associated to the qualitative controller comparison

Index	Value (CRONE)	Value (Benchmark)
$RIAE_1$ (C_2 ,C_1)	0.28196	0.3511
$RIAE_2$ (C_2 ,C_1)	0.2918	0.4458
$RITAE_1$(C_2 ,C_1 ,t_{c1} ,t_{s1})	0.21776	1.6104
$RITAE_2$(C_2 ,C_1 ,t_{c2} ,t_{s2})	0.09181	0.1830
$RITAE_2$(C_2 ,C_1 ,t_{c3} ,t_{s3})	0.13766	0.3196
$RITAE_2$(C_2 ,C_1 ,t_{c4} ,t_{s4})	0.065014	0.1280
$RIAVU_1$ (C_2 ,C_1)	1.0567	1.1283
$RIAVU_2$ (C_2 ,C_1)	1.1143	1.3739
J(C_2 ,C_1)	0.2751	0.68209

6. CONCLUSION

In this paper, we propose a frequency-domain method to design a robust decentralized PID controller for a MIMO refrigeration system based on vapour compression. The designed controller was obtained by optimizing open-loop linear behaviours using the multi-SISO CRONE CSD approach. It took into account both the nonlinear and MIMO behaviours of the plant. Good control performances of the proposed controller have been demonstrated in simulation and compared to another control structure provided by the PID 2018 Benchmark.

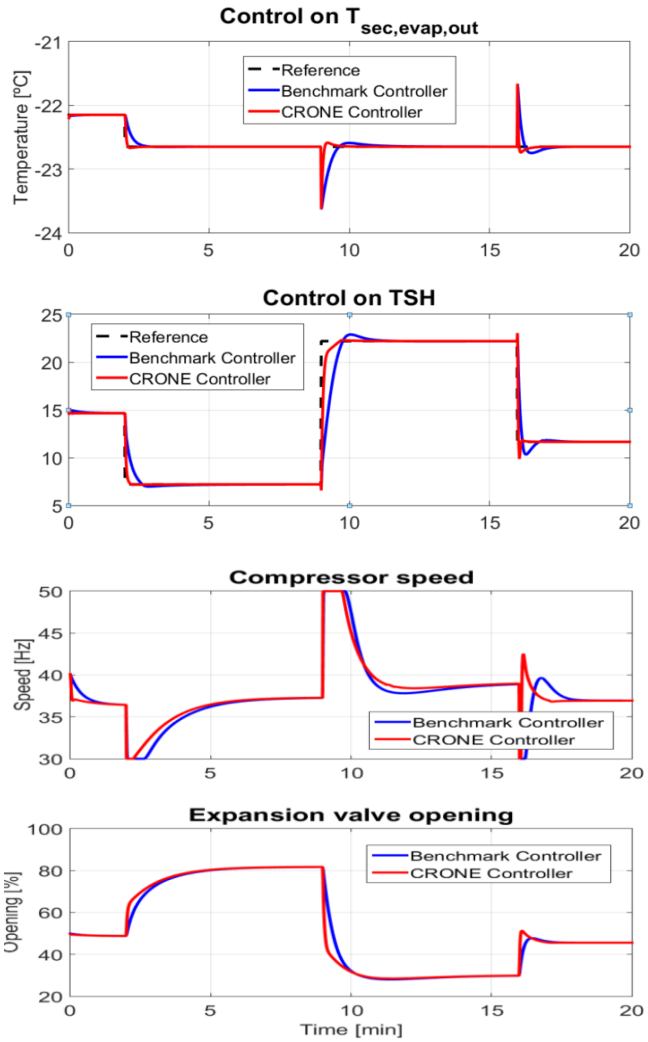

Fig. 12 Qualitative comparison of two standard simulations with the MIMO Refrigeration Control System: controlled and manipulated variables

REFERENCES

Bejarano, G., Alfaya, JA., Rodriguez, D., Ortega, MG., Morilla,F. (2017), Benchmark for PID control of Refrigeration Systems based on Vapour Compression, *3rd IFAC Conference on Advances in Proportional-Integral-Derivative Control*, Ghent , Belgium.

Chen, YQ., Moore, K.L., Vinagre, B. and Podlubny, I. (2004). Robust PID controller autotuning with a phase shaper. In *Proceedings of The First IFAC Symposium on Fractional Differentiation and its Applications* (FDA04), Bordeaux, France

Lanusse, P. (1994), *De la commande CRONE de première génération à la commande CRONE de troisième generation*. PhD Thesis, Bordeaux I University, France.

Lanusse P, Oustaloup A, Sutter D (1996), Multi-scalar CRONE control of multivariable plants, *WAC'96-ISIAC Symphosia,* Montpellier, France.

Lanusse, P., Oustaloup, A., Mathieu, B. (2000), Robust control of LTI square MIMO plants using two CRONE control design approaches, *IFAC Symposium on Robust Control Design "ROCOND 2000"*, Prague, Czech Republic.

Lanusse, P. (2010) CRONE Control System Design, a CRONE toolbox for Matlab, http://www.ims-bordeaux.fr/CRONE/toolbox.

Lanusse, P., Nelson-Gruel, D., Lamara, A. (2016), Toward a CRONE toolbox for the design of full MIMO controllers, *International Conference on Fractional Differentiation and its Applications*, Novi Sad, Serbia.

Lamara, A., Colin, G., Lanusse, P., Chamaillard, Y. and Charlet, A. (2012). Decentralized robust control-system for a non-square MIMO system, the air-path of a turbocharged Diesel engine, *IFAC workshop ECOSM 2012*.

Monje, CA., Chen, Y., Vinagre, BM., Xue, D., Feliu-Batlle, V. (2010). *Fractional-order Systems and Controls: Fundamentals and Applications*, Springer.

Nataraj, PSV. and Tharewal, S. (2007). On fractional-order QFT controllers. *Trans. ASME J. Dynamic Systems, Measurement, and Control*, 129:212–218.

Nelson-Gruel, D., P. Lanusse, A. Oustaloup (2008), Decentralized CRONE control of mxn multivariable system with time-delay, *3nd IFAC Workshop on "Fractional Differentiation and its Applications" (FDA'08)* - Ankara.

Oustaloup, A. (1983), *Systèmes asservis linéaires d'ordre fractionnaire*, Masson, Paris.

Oustaloup, A. (1991). *La commande CRONE*. Hermes Editor, Paris.

Oustaloup, A., Mathieu, B., Lanusse, P. (1995), The CRONE control of resonant plants: application to a flexible transmission, *European Journal of Control*, Vol. 1, n°2, pp. 113-121.

Petras, I. (1999). The fractional-order controllers: methods for their synthesis and application, *Journal of Electrical Engineering*, 50(9-10):284–288.

Podlubny, I. (1999a). *Fractional Differential Equations*, Academic Press, San Diego, CA.

Podlubny, I. (1999b). Fractional-order systems and $PI^{\lambda}D^{\mu}$ controllers, *IEEE Trans. Automatic Control*, 44(1):208–214.

Sabatier, J., Lanusse., Melchior, P., Oustaloup, A. (2015), *Fractional Order Differentation.and Robust Control Design*, Springer Academic edition.

Sutter, D (1997) *La commande CRONE multiscalaire: application à des systèmes mécaniques articulés*, PhD Thesis, Bordeaux I University, France.